Original Article

Better specificity and less ischemia: three-dimensional reconstruction is superior to routine computed tomography angiography in navigation of super-selective clamping robot-assisted laparoscopic partial nephrectomy

Chong Wu[1]#^, Shengjie Guo[1]#, Shuiqing Zhuo[2]#, Yanjun Wang[1], Yunlin Ye[1], Zaishang Li[3,4], Yonggao Mou[5], Xiangyun Yang[1], Zhiling Zhang[1], Pei Dong[1], Fangjian Zhou[1], Hui Han[1]

[1]Department of Urology, Sun Yat-sen University Cancer Center, State Key Laboratory of Oncology in South China, Collaborative Innovation Center for Cancer Medicine, Sun Yat-sen University, Guangzhou, China; [2]Department of Radiology, Sun Yat-sen University Cancer Center, Guangzhou, State Key Laboratory of Oncology in South China, Collaborative Innovation Center for Cancer Medicine, Sun Yat-sen University, Guangzhou, China; [3]Department of Urology, Shenzhen People's Hospital, The Second Clinic Medical College of Jinan University, Shenzhen, China; [4]Department of Urology, First Affiliated Hospital of Southern University of Science and Technology, Minimally Invasive Urology of Shenzhen Research and Development Center of Medical Engineering and Technology, Shenzhen, China; [5]Department of Neurosurgery/Neuro-oncology, Sun Yat-sen University Cancer Center, State Key Laboratory of Oncology in South China, Collaborative Innovation Center for Cancer Medicine, Sun Yat-sen University, Guangzhou, China

Contributions: (I) Conception and design: H Han, C Wu; (II) Administrative support: F Zhou; (III) Provision of study materials or patients: S Zhuo, Y Wang; (IV) Collection and assembly of data: S Guo, S Zhuo, C Wu; (V) Data analysis and interpretation: H Han, C Wu; (VI) Manuscript writing: All authors; (VII) Final approval of manuscript: All authors.

#These authors contributed equally to this work.

Correspondence to: Hui Han. Sun Yat-sen University Cancer Center, 651 Dongfengdonglu, Guangzhou 510060, China. Email: hanhui@sysucc.org.cn.

Background: Available technologies could be used to guide surgeons in controlling highly selective tumor-bearing arteries robot-assisted laparoscopic partial nephrectomy (RALPN).

Methods: Patients undergoing RALPN (from September 2018 to January 2020) for intermediate-high complex renal tumor (R.E.N.A.L. score ≥7) who underwent abdominal computed tomography (CT) scan with angiography and hyper-accuracy 3-dimensional reconstruction (H3DR). All patients underwent high-resolution CT scan with angiography and H3DR with special software, based on which two kinds of highly selective arterial clamp protocols were made for each patient and analyzed independently by two urologists and two radiologists to confirm which renal arterial branch was supplying the tumor. We chose the optimized clamping protocol with the principle of the minimized ischemic regions. During the operation, meticulous microdissection and clip ligation of the specific vascular branch was guided by optimized protocol [H3DR or computed tomography angiography (CTA) reconstruction], according to the *in vivo* anatomy (identified by intraoperative ultrasound).

Results: Of 82 patients, the minimum-ischemic regions planning completed rate (MIRPCR) of preoperative planning with H3DR (90.2%) was higher than that with CTA (34.1%) (P<0.01). H3DR identified 78 high-order arteries (70.3%), whereas CTA identified 33 (29.7%) high-order arteries (P<0.001). H3DR detected a more optimal blocking option in 51 cases that were either missed (n=13) or misclassified by CTA (n=38). A total of 18 cases (56.3%) were converted to H3DR-guided occurred in CTA-guided surgery [5 (10.0%) occurred in group H3DR to CTA, P<0.01]. Moreover, in the CTA-guided group, the separation of renal hilum was avoided in 14 of 19 (73.7%) cases, whereas in the H3DR-guided group, it was avoided in 60 of 63 (95.3%) cases.

^ ORCID: 0000-0003-0671-4365.

Conclusions: For patients undergoing RALPN, H3DR-guided surgery compared with standard CTA-guided surgery has higher accuracy and feasibility in controlling arterial branches supplying the tumor and intraoperative surgical navigation. Additionally, it reduces the ischemic lesion area and simplifies vascular isolation steps, thus decreasing procedural difficulty.

Keywords: Three-dimensional reconstruction-guided surgery; zero-ischemia; partial nephrectomy (PN); robotics

Introduction

Partial nephrectomy (PN) should entail optimal locoregional tumor control with minimization of procedure-related complications (1). The impact of ischemic injury on renal function remains controversial (2-6). Many studies concur on the two main principles regarding the optimization of functional outcomes: maximizing parenchymal volume preservation and minimizing ischemia-related nephron damage (7-10).

By identifying the unique blood supply of the renal mass, global ischemia to the healthy remnant may be avoided. Thus, several techniques of selective renal ischemia have been described (11,12) (e.g., minimal ischemia or zero ischemia). Recently, minimizing warm ischemia injury has been a surgical focus with an aim to maximize the preservation of nephron units, and the technique of segmental renal artery clamping has emerged as a promising method for renal hilar control. Conventional computed tomography angiography (CTA) (13,14) of the kidney based on CT scan images is a routinely used tool during selective arterial clamping PN. Meanwhile, planning graph-derived guidance to target arteries based on hyper-accuracy 3-dimensional reconstruction (H3DR) of anatomic renal structures from CT scan images and bidimensional CT scan slices has been evaluated (15-20) as a tool of intraoperative arterial segmental dissection navigation.

Due to the high variability in the renal vasculature and tumors, a useful delineation of the lesion and the relation to anatomical structures should undoubtedly be provided. H3DR, fused with 3-dimensional (3D) images of the surface-rendered renal tumor and semitransparent kidney, has facilitated selective microdissection of tumor-specific arterial branches during zero-ischemia PN (15,17,18,20).

With the advent of the da Vinci Surgical System, its numerous advantages such as superior image magnification, 3D imaging, 7-degree-of-freedom wristed devices, tremor filtering and shortened learning curve (21), has made minimally invasive PN a feasible option even for highly complex renal masses. robot-assisted laparoscopic partial nephrectomy (RALPN) is considered as a feasible and effective alternative to open and laparoscopic PN in the treatment of complex renal tumors (22-24).

Comparisons of CTA- and H3DR-guided surgery protocols for the RALPN with selective clamp have shown that the H3DR virtual-navigation technique allows for a more accurate representation of the kidney arterial vasculature than CTA (25,26). Although H3DR is an appealing pathway, few data support its reliability. The precise mechanism of the H3DR advantage is not yet known and it is unclear what proportion and what grade of tumor-feeding vessel would be misidentified by CTA-guided planning. With this in mind, we designed a prospective control study to compare H3DR- and CTA-guided surgery in patients with localized intermediate-to-high complex renal tumor. The primary outcome was

---

Highlight box

Key findings
- H3D reconstruction offers precise intraoperative surgical navigation in RALPN.

What is known and what is new?
- 3D image-guided surgery could avoid global ischemia following the removal of a renal tumor.
- H3DR-guided-surgery, compared with standard CTA-guided surgery, has higher accuracy and feasibility in controlling arterial branches supplying the tumor and intraoperative surgical navigation.

What is the implication, and what should change now?
- H3DR-guided surgery protocols should be actively introduced in the clinic for the development of individualized surgery with better precision.

the minimum-ischemic regions planning completed rate (MIRPCR) between CTA- and H3DR-guided RALPN, and the secondary outcomes included the proportion of high-order vessel (the 3rd- and 4th-order branch of the main renal artery) planning, conversion rate (CTA conversion to H3DR or H3DR conversion to CTA), and hilar separation rate during operation. We present the following article in accordance with the STROBE reporting checklist (available at https://tau.amegroups.com/article/view/10.21037/tau-22-865/rc).

Methods

Patients were recruited from Sun Yat-sen University Cancer Center from September 2018 to January 2020. Our center performed >500 RALPN over each of these years. The study was conducted in accordance with the Declaration of Helsinki (as revised in 2013). Patient data were prospectively collected, and the study was approved by Sun Yat-sen University Cancer Center Ethics Committee (approval number XJS2018-005-01), and informed consent was taken from all the patients. Before the intervention, all patients underwent a high-resolution abdominal CT scan and H3DR reconstruction.

Inclusion/exclusion criteria

Patients with clinical stage T1N0M0 moderate or complex renal tumors (R.E.N.A.L. score ≥7) were deemed to be candidates for RALPN. The exclusion criteria were severe cardiopulmonary or cerebrovascular disease, aged over 80 years, life expectancy of less than 5 years, horseshoe kidney, renal duplication, evidence of perinephric adhesion or previous kidney surgery, which would have increased the difficulty of separating the renal vasculature.

CTA and 3D reconstruction protocol

All 82 patients underwent renal CT scans using a Siemens Dual-source CT instrument (SOMATOM Force CT, Siemens, Erlangen, Germany) with dual-energy scanning mode. CT images were acquired with double-tube tube: voltage/tube current: 100 kV/ref250 mAs (tube A) and Sn150 kV/ref125 mAs (tube B); rotation speed 0.5 s; pitch of 1; collimation width was 2×192×0.6 mm and slice width was 1 mm. The images were divided automatically into two sets (A and B). The patients adopted the supine position. A high-pressure syringe (Stellant; Medrad, Pittsburg, PA,

USA) was used to administer nonionic iodine contrast material containing 370 mg I/mL at a rate of 4 mL/s to all patients. Contrast media intelligent tracking technology was adopted when the tracking point was 2 mm under the diaphragm at the abdominal aorta level. The area of regions of interest (ROI) was 1 mm^2 and bolus tracking was used to initiate the automatic scan once the trigger threshold of 100 HU was reached (delay, 7 sec). Approximately 20 mm below the diaphragm to the level of the anterior superior iliac spine were scanned. The scanned images were transmitted to the processing workstation and 3D reconstructions of the images were generated using Syngo via software (Siemens, Germany). CTA images were generated after post-processing by maximum intensity projection (MIP) and volume rendering technique (VRT).

Based on the data from CT examination, images in Digital Imaging and Communications in Medicine format (DICOM) were processed by dedicated software (Urinary Image Processing Software 1.8; Hubei INCOOL Science & Technology Co., Ltd., Wuhan, China). H3DR was jointly performed by an experienced radiologist and a professional technical engineer. Reconstruction of 3D images allowed us to merge critical anatomic structures including renal mass, semitransparent renal parenchyma, vasculature, and collecting systems. For segmentation of the kidney surface, arterial phase images with automated thresholding were used, and for reconstructed renal pedicles, the dynamic region growing method was applied, as well as tumor-specific blood vessels. Next, 3D images and models were created. Also, the feeding artery was marked in different color for discrimination. An analysis of the renal tumor feeding arteries was performed using the two imaging modalities, matched with intraoperative RALPN observations.

The concept and classification of MIRPC

The clamping approach, based on CTA or H3DR, may show differences (or the same) when displaying the intrarenal anatomy of the collecting system and vessels, resulting in different (or the same) presurgical clamp plans in the same patient. Thus, during operation, we chose the clamping scheme approach prioritizing minimization of ischemic regions (patients were assigned to different groups according to preoperative vascular planning, see *Figure 1*). If there were failed attempts with the first approach, the procedure was converted to the other approach. The MIRPCR was defined as the proportion of optimal
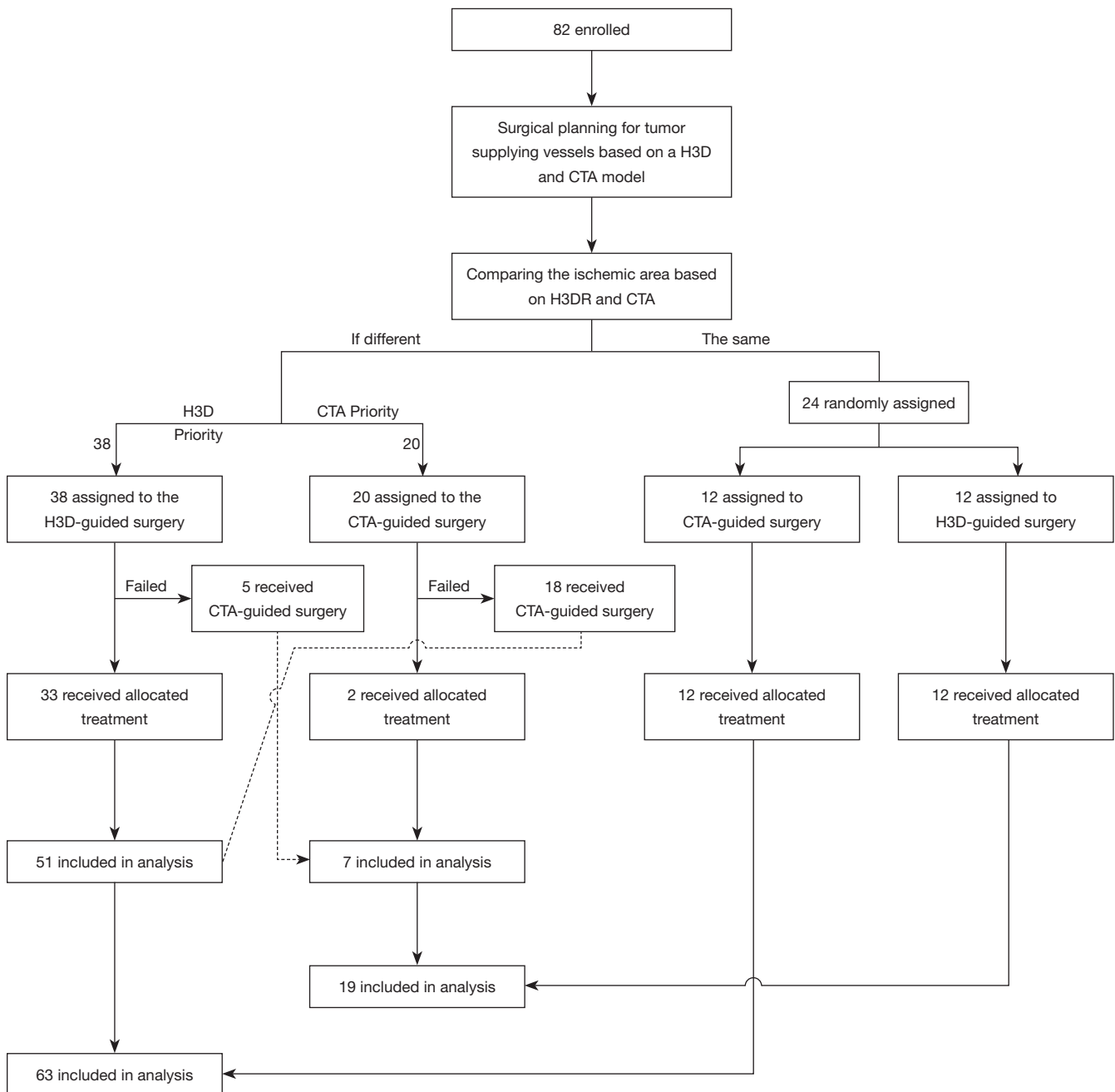
Figure 1 Flow diagram depicting the design of the control study showing H3DR pathway- and standard CTA-guided surgery. H3DR, hyper-accuracy 3-dimensional reconstruction; CTA, computed tomography angiography.

vascular-locked planning being completed, and it was calculated as follows: MIRPCR$_{\text{CTA or H3DR}}$ (%) = (number of cases successfully completed by CTA or H3DR)/82. A successfully completed case was defined when intraoperative management of the renal pedicle was conducted as preoperatively planned.

Procedures

Preoperative management

All patients underwent CTA and H3DR with special software. Before the surgery, two kinds of highly selective arterial clamp plans, based on CTA and H3DR, were
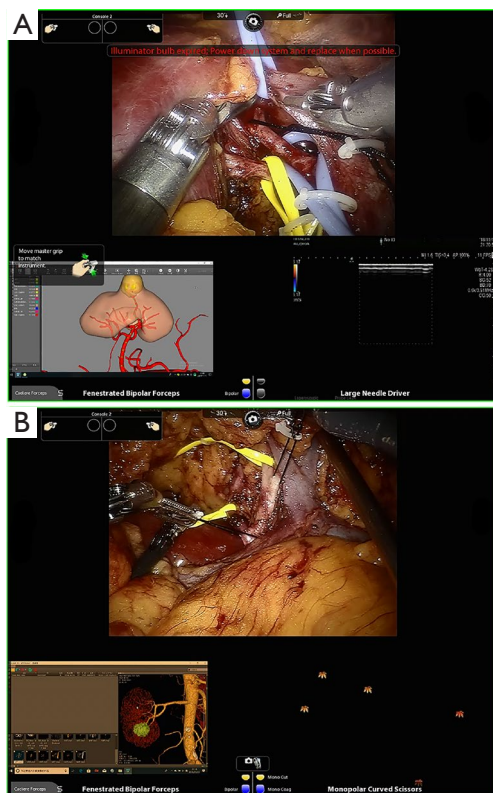
Figure 2 3-dimensional reconstruction model of the tumor were shown on the da Vinci surgical system's display screen: (A) H3DR pathway; (B) standard CTA guided surgery. H3DR, hyper-accuracy 3-dimensional reconstruction; CTA, computed tomography angiography.

made for each patient and analyzed independently by two urologists and two radiologists for confirmation of the vessels supplying the tumor. During the operation, dissection of the target artery was guided by H3DR or CTA reconstruction alternatively, with manual orientation by the assistant or surgeon. We chose the clamping scheme/approach with priority of minimized ischemic regions. If there were failed attempts with the first approach, the procedure was converted to the alternative approach. The aim of precise clamping was to produce a minimal ischemic area, yet still be sufficient to control bleeding from the defect (details of the practical flow chart are shown in *Figure 1*).

All the procedures were performed by a single experienced surgeon (Dr H.H, experience with over 500 RALPN procedures). After the blocking site of tumor blood supply vessels was identified, the choice of surgical approach depended on the location of the tumor/segmental arterial and the experience of the surgeon. Then, the target vessels were marked preoperatively with the reference to a CTA or 3D anatomical model.

Surgical procedures

After Gerota's fascia lata was exposed, dissection of the target segmental vessel was carried out from the renal sinus or following the segmental renal artery nearest to the target vessel as anticipated by H3DR reconstruction or CTA. A derivation graph of H3DR or CTA via interface of Davinci system console input (Tile-pro display) could be manipulated dynamically when needed and showed the picture from multi-angle directions to help the surgeon to specifically target the segmental arteries. Guided by 3D reconstruction, the renal vein or its branch, ureter, segmental arteries (1st–3rd order or higher), extra exophytic renal cyst, collecting system, as well as tumor location and their anatomic relative locations could be orientated as reference points more conveniently than by CTA images. The dissection of the renal vessel ended with the identification of the branch/branches of the target artery supplying the tumor (*Figure 2*).

Routine use of the Davinci third arm could help to pull surrounding tissues around the target vessel and separate the high order artery effectively. For the higher-order branch of the main renal artery, we changed the needle holder to separate, taking care to avoid injuring the vasculature (*Figure 2A*).

Intraoperative ultrasonography (Hitachi Ltd., Tokyo, Japan) was routinely used to determine tumor dimensions, location, and blood flow. A microsurgical bulldog clamp was placed to block blood flow as described elsewhere (19). Doppler ultrasonography was carried out during the operation to test the tumor and renal parenchyma flow (*Figure 3*, Video S1). Subsequently, enucleoresection or enucleation was carried out according to clinical indication, and intermittent use of suction and irrigation provided a clear surgical field for the surgeon. If the urinary collecting system was cut open (>3 mm), indigo carmine mixed with saline was injected through the preoperatively placed ureteral catheter to visualize apertures of the collecting system. The collecting system entry was closed in a watertight manner. Methylene blue was routinely used intraoperatively to check for any evidence of incision leakage.
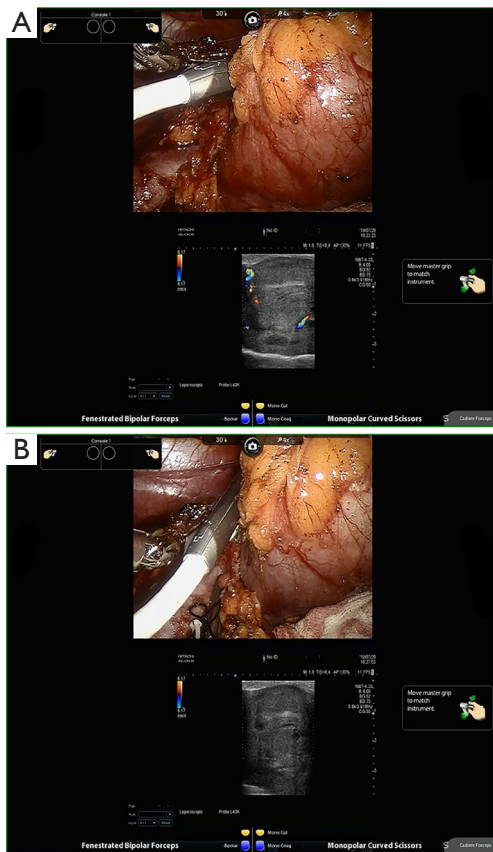
Transl Androl Urol 2023;12(1):97-111 | https://dx.doi.org/10.21037/tau-22-865

102

Wu et al. Zero ischemia techniques in partial nephrectomy surgery

Figure 3 Intraoperative color Doppler ultrasound was used to determine blockade of blood flow of renal tumor (controlling higher-order arterial branches) during (A) the pre-clamp and (B) clamp period.

Outcome measures and data collection

We collected demographic information for each patient, including age, body mass index (BMI), medical history, physical examination, serum creatinine (sCr), split renal function (SRF), and estimated glomerular filtration rate (eGFR) calculated using the modification of diet in renal disease (MDRD) formula, and the R.E.N.A.L. nephrometry score for assessing the complexity of a renal mass (27); perioperative data (including management of the renal pedicle, type and duration of ischemia; and Our study assessed the compliance rate of the preoperatively planned management of renal pedicles after the surgery specifically for this purpose); pathological data [including stage according to tumor-node-metastasis (TNM) (28)]; Clavien-Dindo classification of postoperative complications (29); and follow-up data (including serum creatinine, SRF measured

by radionuclide renogram, an abdominal evaluation using ultrasound or CT scan; The patient was referred for an elective bone scanning, chest CT imaging, and magnetic resonance imaging (MRI) when clinically indicated.

The assessment of renal function included sCr, eGFR, the SRF, and functional kidney volume (FKV). We measured sCr preoperatively, 3 hours after the procedure, on the day of discharge, and 3 months postoperatively. Evaluation of postoperative renal function included change in eGFR and incidence of acute kidney injury (AKI). AKI was defined as a >25% change in eGFR within 3 days of surgery. The prevalence of new-onset chronic kidney disease (CKD) was assessed using an eGFR <60 mL/min/1.73. The SRF was measured by radionuclide renogram in all cases preoperatively and 3 months after the operation.

Tumor-specific feeding arteries were measured preoperatively from conventional CTA and H3DR. After the number and order of planned segmental arterials were obtained, for the purposes of the experiment, this dataset was divided into two groups: H3DR and CTA planning data sets. The percent of each-order planned branches based on CTA and H3DR was the proportion of x-order (x= I, II, III, IV) planned branches (CTA or H3DR) out of total x-order (x= I, II, III, IV) planned branches (CTA and H3DR).

The first- and second-order branch of the main renal artery were defined as lower-order arteries. Similarly, the tertiary- and quaternary-order branch (or higher) of the main renal artery were defined as higher-order arteries.

Statistical analysis

Frequencies and proportions (e.g., the minimum-ischemic regions planning coincidence rate, the higher-order vessel planning rate) were compared using chi-square test. The means of continuous outcomes (e.g., zero ischemia time, operating time, sCr, eGFR, and length of postoperative hospitalization) were compared using Student's t-test. A P value <0.05 was considered statistically significant.

Results

Patient recruitment and baseline characteristics

A total of 82 patients underwent highly selective clamping RALPN successfully through the retroperitoneal approach (30 cases), transperitoneal approach (50 cases), and combined approach (2 cases). A total of 82 eligible patients underwent their assigned interventions and formed the

Table 1 Clinicopathologic features and preoperative planning outcomes

Variable	CTA-guided surgery (N=19)	H3D-guided surgery (N=63)	P value
Age (year), median (IQR)	50 [46–58]	50 [41–60]	–
Male, n (%)	11 (64.6)	42 (64.6)	0.43
BMI (kg/m^2), median (IQR)	23.4 (21.4–26.4)	24.0 (22.5–25.5)	0.80
Tumor size at CT scan (cm), median (IQR)	3.5 (2.8–4.3)	4.0 (3.2–4.9)	0.51
Preoperative CKD stage, n (%)			0.17
≤1	9 (47.4)	39 (61.9)	–
2	10 (52.6)	21 (33.3)	–
3	0 (0.0)	3 (4.8)	–
ASA score, n (%)			0.50
1	5 (26.3)	20 (31.7)	–
2	14 (73.7)	41 (65.0)	–
3	0 (0.0)	2 (3.3)	–
Laterality, n (%)			0.40
Right	11 (57.8)	43 (68.2)	–
Left	8 (42.2)	20 (31.8)	–
RENAL score, n (%)			0.85
7	4 (21.0)	9 (14.4)	–
8	5 (26.3)	17 (26.8)	–
9	4 (21.0)	18 (28.6)	–
10	5 (26.3)	17 (26.8)	–
11	1 (2.5)	1 (1.7)	–
12	0 (2.9)	1 (1.7)	–

IQR, interquartile range; BMI, body mass index; CKD, chronic kidney disease; CT, computed tomography; ASA, American Society of Anesthesiologists; RENAL, Radius, Exophytic/endophytic, Nearness, Anterior/posterior, Location; CTA, computed tomography angiography; H3D, hyper-accuracy three-dimensional.

preparatory surgery population (20 in the CTA-guided surgery group, 38 in the H3DR-guided surgery group, and 24 in the random group; *Figure 1*). A total of 24 patients in the random group underwent randomization (12 in the CTA-guided group and 12 in the H3DR-guided group). In the H3DR-guided surgery group, 5 [10.0%=5/(12+38)] patients were converted to the CTA-guided surgery group because the target vessel was too hard to separate or the blood flow was not blocked completely after the target artery was occluded with the micro bulldog clamp, as assessed by intraoperative doppler ultrasonography. Similarly, 18 [56.3%=18/(12+20)] patients in the CTA-guided surgery group were converted to the H3DR-guided

surgery group. Ultimately, our study included 19 patients in the CTA-guided surgery group and 63 in the H3DR-guided surgery group. These patients were included in the final analysis according to the regimens that they finally received. Patient demographics and preoperative characteristics are shown in *Table 1*. Perioperative variables are reported in *Table 2*.

Comparison of MIRPCR of CTA and H3DR-guided surgery and preoperative planning outcomes

The MIRPCR of preoperative planning with H3DR (90.2%) was higher than that with CTA (34.1%; P<0.01)

Table 2 Perioperative variables

Variable	Total (N=82)	CTA-guided surgery (N=19)	H3D-guided surgery (N=63)	P value
Trifecta achievement, n (%)	37 (45.1)	9 (47.3)	28 (44.4)	0.734
Indwelling ureteral catheter, n (%)	16 (19.5)	5 (26.3)	11 (17.4)	0.405
Hospital stay (d), median (range)	4.9 [2–11]	5.9 [4–11]	4.6 [2–10]	<0.001
Clamping of renal artery, n (%)				
Global ischemia	0 (0.0)	0 (0.0)	0 (0.0)	–
Selective ischaemia	82 (100.0)	19 (100.0)	63 (100.0)	–
Surgical approach, n (%)				0.558
Transperitoneal	50 (61.0)	12 (63.1)	38 (60.3)	–
Retroperitoneal	30 (36.6)	7 (36.8)	23 (36.5)	–
Combined	2 (2.4)	0 (0.0)	2 (3.2)	–
No. of openings of the collecting system (%)	31 (37.8)	7 (36.8)	24 (36.5)	0.921
MIRPCR, n (%)	–	28 (34.1)	74 (90.2)	<0.001
No. of conversion to H3D-guided (%)	–	18 (56.3)	–	<0.01
No. of conversion to CTA-guided (%)	–	–	5 (10.0)	–
The separation of renal hilum, n (%)	–	5/19 (26.3)	3/63 (4.7)	0.011
Use of intraoperative US, n (%)	82 (100.0)	82 (100.0)	82 (100.0)	–
Zero ischemia time (min), mean (SD)	29.8 (12.8)	30.8 (16.3)	29.4 (11.5)	0.152
EBL (mL), mean (SD)	289.0 (304.5)	255.7 (327.2)	299.0 (299.3)	0.893
Operative time (min), mean (SD)	122.2 (45.3)	120.2 (52.0)	122.8 (43.5)	0.943
No. of intraoperative complications (%)	0 (0.0)	0 (0.0)	0 (0.0)	–
No. of transfusions (%)	4 (4.8)	1 (5.2)	3 (4.7)	0.729
No. of conversion to radical nephrectomy (%)	0 (0.0)	0 (0.0)	0 (0.0)	–
No. of postoperative complications, Clavien (%)				0.246
<3	14 (17.0)	2 (10.5)	12 (19.0)	–
≥3	5 (6.0)	2 (10.5)	3 (4.7)	–
Complication surgery related, n (%)				
Urine leak	5 (6.0)	2 (10.5)	3 (4.7)	0.386
Poor wound healing	1 (1.2)	0 (0.0)	1 (1.5)	0.466
AKI, n (%)				
RIFLE criteria	9 (12.5)	1 (5.2)	8 (12.7)	0.329
Risk	6 (7.3)	0 (0.0)	6 (9.5)	0.069
Injury	2 (2.4)	1 (5.2)	1 (1.5)	0.403
Failure	1 (1.2)	0 (0.0)	1 (1.5)	0.466
KDIGO	10 (12.2)	1 (5.2)	9 (14.3)	0.254
1	4 (4.8)	0 (0.0)	6 (9.5)	0.069
2	2 (2.4)	1 (5.2)	1 (1.6)	0.403
3	1 (1.2)	0 (0.0)	2 (3.2)	0.301

MIRPCR, minimum-ischemic regions planning completed rate; CTA, computed tomography angiography; H3D, hyper-accuracy three-dimensional; US, ultrasound; SD, standard deviation; EBL, estimated blood loss; AKI, acute kidney injury; RIFLE, risk, injury, failure, loss, end-stage (renal); KDIGO, Kidney Disease: Improving Global Outcomes.

Table 3 Comparison of preoperative planning outcomes with CTA and H3D

Variable	Cases No.	Total vessel numbers	Lower-order arterial branches			Higher-order arterial branches		
			I order	II order	Total	III order	IV order	Total
CTA	82	114	30	51	81	28	5	33
H3D		131	14	39	53	63	15	78
Total	–	245	44	90	134	91	20	111
Difference, %	–	+20.4	−53.3	−23.5	–	+125.0	+200.0	–

CTA, computed tomography angiography; H3D, hyper-accuracy three-dimensional.

(*Table 2*). Of the 245 vessels identified by CTA and H3DR preoperatively, 114 and 131 were derived from CTA and H3DR, respectively. Of these, 111 (45.3%) were high-order arteries; 134 (54.7%) were low-order arteries. Besides, we found that H3DR identified 78 (70.3%=78/111) high-order arteries; CTA identified 33 (29.7%=33/111) high-order arteries (P<0.01) (*Table 3*). H3DR detected more optimal blocking option in 51 cases that were either missed (n=13) or misclassified by CTA (n=38) (Table S1). In the 13 cases and 15 arteries missed by CTA, the grades were II-order (n=1), III-order (n=3), IV-order (n=8), and V-order (n=3). In the misclassified cohort, classification adjustment as high order in 7 patients and as low order in 31 patients. In the CTA-guided group, the separation of renal hilum was avoided in 13 of 17 (76.4%) cases, whereas in the H3DR-guided group, it was avoided in 60 of 63 (95.2%) cases. The discordance analysis is presented in Table S1. CTA detected the optimal target artery in 5 men who were over-diagnosed with H3DR.

Postoperative complications and renal function

There were no intraoperative complications. Overall, the postoperative complication rate was 23.1%. Of these, 14 were low grade (Clavien-Dindo grade 1 to 2), including 4 (5.3%) cases of postoperative bleeding, 2 urine leaks that resolved spontaneously without intervention, and 8 patients who received sedative and analgesic medications and medication for pain treatment. High-grade complications (Clavien-Dindo grade 3 or greater) occurred in 5 patients (6.1%). In 1 of these patients, there was a pulmonary embolism requiring thrombolytic treatment in the intensive care unit (ICU), and another patient was treated with debridement and suturing under general anesthesia for poor wound healing. There were 3 patients with urine leakage that required stenting of the ureter. A total of 4 patients

(4.9%) required postoperative transfusion and a transfusion of 13 units of red cell concentrate was given to these patients (*Table 2*).

The renal functional outcome evaluation showed postoperative (at last follow-up) worsening of ΔeGFR equal to –0.4% and 9.8% (P<0.05), with ΔGFR values of 9.8% and 9.1% (P>0.05), in the CTA and H3DR-guided surgery groups, respectively (*Table 4*). A total of 18 patients developed new-onset CKD (15 in H3DR and 3 in CTA), and 5 patients developed CKD progression at last follow-up (all in H3DR). The pathological data are reported in *Table 5*. There were two positive surgical margins recorded.

Discussion

There are two main points to consider when evaluating residual renal function after PN: renal parenchyma residual volume and renal ischemia injury. Prior studies have noted the importance of the effect of warm ischemia on renal function. It has been suggested that impairment in renal function following a limited warm ischemia time (WIT) of Some experts suggested that it is temporary and spontaneously reversible to have a limited warm ischemia time (WIT) of 30 minutes; however, Thompson *et al.* (30) suggest that if the renal hilum is clamped, every minute counts, especially if the patient has pre-existing complications or underlying renal dysfunction. Hilar clamping inevitably inflicts ischemic injury on the kidney.

Initially, some studies proposed the zero-ischemia LPN concept (17,18). An attempt was made to eliminate global renal ischemia by microdissecting tertiary or quaternary renal artery feeding the tumor, based on the concept of anatomical renovascular microdissection and CTA guidance (13,14,19). However, this is technically challenging and was not widely implemented.

With the development of technology, conventional

Table 4 Functional variables

Variable	CTA-guided surgery	H3D-guided surgery	P value
Preoperative SCr (μmol/L), mean (SD)	65.7 (18.7)	72.4 (23.4)	0.259
Preoperative eGFR (mL/min), mean (SD)	109.5 (22.9)	103.5 (25.6)	0.361
Postoperative SCr (μmol/L), mean (SD)	72.2 (18.9)	79.5 (26.7)	0.299
Postoperative eGFR (mL/min), mean (SD)	110.0 (25.4)	93.3 (24.6)	0.019
ΔSCr (%)	+7.6	+12.7	0.488
ΔeGFR (%)	+0.4	−9.8	0.793
Preoperative GFR (mL/min), mean (SD)	96.2 (21.2)	93.2 (26.7)	0.670
Preoperative ipsilateral side (mL/min), mean (SD)	50.3 (10.9)	46.0 (12.6)	0.210
Preoperative contralateral side (mL/min), mean (SD)	45.9 (14.5)	47.2 (15.0)	0.755
Postoperative GFR (mL/min), mean (SD)	85.1 (20.6)	81.9 (24.4)	0.630
Postoperative ipsilateral side (mL/min), mean (SD)	38.3 (11.1)	35.6 (11.0)	0.402
Postoperative contralateral side (mL/min), mean (SD)	46.7 (14.6)	47.1 (13.3)	0.928
ΔGFR (%)	−9.8	−9.1	0.998
ΔGFR (ipsilateral side) (%)	−23.8	−22.6	0.761
ΔGFR (contralateral side) (%)	+1.7	−0.2	0.965

CTA, computed tomography angiography; H3D, hyper-accuracy three-dimensional; eGFR, estimated glomerular filtration rate; GFR, glomerular filtration rate; SCr, serum creatinine.

CTA models allow a reliable and accurate visualization of the respective organ (renal tumor, vasculature, and renal parenchyma). Due to the opaque nature of the CTA reconstructed images, only the extrarenal vasculature could be easily visualized. However, it cannot present organs simultaneously (e.g., renal arteries and veins) and create arbitrary combinations (any 2 or more organs model can be combined arbitrarily). Indeed, conventional CT prevents the detailed knowledge of the number and location of intrarenal tumor feeding arteries, and their relationship with the collecting system, prior to surgery. Some attempts have been made with H3DR reconstruction techniques. Studies (15,17,18) performed zero-ischemia PN without hilar clamping in 57 patients and concluded that global surgical renal ischemia is unnecessary for the majority of patients undergoing robotic/laparoscopic PN. Recent studies support the superiority of H3DR-guided surgery to evaluate the surgical complexity, decrease operative time, patient length of stay, and the rate of global ischemia, as well as increase the concordance rate of preoperative planning (31). Porpiglia *et al.* (25,26) found that in the H3DR group, a significantly lower number of patients experienced global ischemia (24% *vs.* 80%, P<0.01). These

studies are limited by the use of matched cohorts instead of a single cohort or did not conduct a full comparison of the planning and surgery processes, which are both strong points of our study.

The strength of our study included the in-depth analysis of the difference between H3DR and standard CTA as intraoperative guidance during RAPN in cases of moderate or complex tumors. Most importantly, the MIRPCR of preoperative planning with H3DR (90.0%) was higher than it was with CTA (35.0%) (P<0.01). Secondly, when using the H3DR instead of CTA, the number of tumor-feeding arteries identified as higher-order was greater. This illustrates the accuracy of H3DR in identifying tumor feeding arteries. Thirdly, the isolation of hilar renal vessels is avoided in 74 of 82 (90.2%) cases by landmark guidance of the renal vein or collecting system. In the CTA-guided group, the separation of renal hilum was avoided in 14 of 19 (73.7%) cases, whereas in the H3DR-guided group, it was avoided in 60 of 63 (95.2%) cases (P<0.05).

H3DR is different from conventional CTA in several key respects. Of note, the MIRPCR of preoperative planning with H3DR (90.2%) was higher than with CTA (32.9%) (P<0.01). High MIRPCR of H3DR may be explained by

Table 5 Pathology data

Variable	CTA-guided surgery	H3D-guided surgery	P value
Patients, n (%)	19 (39.0)	63 (61.0)	–
Malignant, n (%)	16 (84.2)	57 (90.5)	0.461
Pathological stage, n (%)			0.325
Benign	3 (15.8)	6 (9.5)	–
pT1a	11 (57.9)	38 (60.3)	–
pT1b	4 (21.0)	16 (25.4)	–
pT2a	1 (5.3)	1 (1.6)	–
pT3	0 (0.0)	2 (3.2)	–
No. of positive surgical margin, n (%)	1 (5.3)	1 (1.6)	0.403
Histology, n (%)			0.584
Clear cell carcinoma	12 (63.2)	40 (63.5)	–
Papillary	1 (5.3)	2 (1.6)	–
Chromophobe	3 (15.75)	10 (15.9)	–
Angiomyolipoma	3 (5.75)	8 (12.7)	–
Other	0 (0.0)	4 (6.3)	–
ISUP grade, n (%)			0.664
1	1 (7.7)	3 (7.5)	–
2	9 (69.2)	30 (75.0)	–
3	3 (23.1)	7 (17.5)	–
4	0 (0.0)	0 (0.0)	–

CTA, computed tomography angiography; H3D, hyper-accuracy three-dimensional; ISUP, International Society of Urological Pathology.

the fact that H3DR may mimic the actual conditions in the renal vasculature and collecting system and can be summarized in three points: (I) semitransparent kidney and 3D course of extra- and intra-renal arteries to allow viewing of embedded structures, which aided identification of the target tumor-feeding artery more precisely; (II) physical occlusion effect, the vessel's block point may be occluded by surrounding tissues, which cannot be clearly displayed in the conventional CTA-guided group; (III) arbitrary combinations, the model could be rotated and zoomed in standard software, and the surgeon could show or hide each anatomic structure during the viewing session. Besides, the higher-order branch (the 3rd- or 4th-order arterial branches of the main renal artery) planning rate was higher (P=0.0159)

in the H3DR planning group. This means that H3DR has higher accuracy and specificity in identifying tumor-specific vessels for selective clamping from the above results.

Several studies have reported that the separation of the higher-order artery from the main artery to the tumor feeding artery remains challenging and time-consuming due to the shelter from the vein, pelvis or ureter, and long dissection distance (15,17,18,25,26). If the renal artery is separated from the main renal arteries to a higher-order branch of the main renal artery by intraperitoneal approach, it needs to be separated behind the renal vein, which is a demanding endeavor with hazards and technical challenges. The H3DR showed the relationship between the target artery and the surrounding anatomy, and the isolation of the segmental renal artery could directly begin from the renal sinus based on the anatomical landmarks to dissect the target blood vessel (for example, from 2nd to 3rd order) instead of exposing the kidney and renal hilum through standard surgical techniques (see *Figure 4*). In contrast, CTA images often have difficulty in delivering more anatomic landmarks precisely (e.g., renal vein and collecting system). Thus, we performed target vessels dissection directly without the renal hilum dissection by taking advantage of its anatomic landmark orientation (see *Figure 4*) of surrounding organs, avoiding accidental damage to surrounding organs. In our study, isolation and clamping of hilar renal vessels were avoided in most cases. In the CTA-guided group, the separation of renal hilum was avoided in 13 of 17 (76.4%) cases, whereas in the H3DR-guided group, it was avoided in 60 of 63 (95.2%) cases.

The following limitations should be acknowledged. The main limitation of this study is that identifying the tumor-feeding artery might have been influenced by subjective bias, which could affect the accuracy of the results. To avoid this problem, all patients' models were constructed by the same radiology and model building team.

Second, the sample size of our study was relatively small. It will be necessary to conduct a prospective, multi-center diagnostic study with larger sample sizes in order to evaluate further the true benefit of H3DR technology compared to standard CTA. Third, although the short-term functional outcomes of selective ischemia PN are encouraging, further studies, involving larger numbers of patients and longer follow-up periods, are required to assess long term renal function and efficacy of super-selective RALPN for patients with cT1N0M0 moderate or complex renal tumors (R.E.N.A.L. score ≥7).

Notwithstanding these limitations, this study is the first
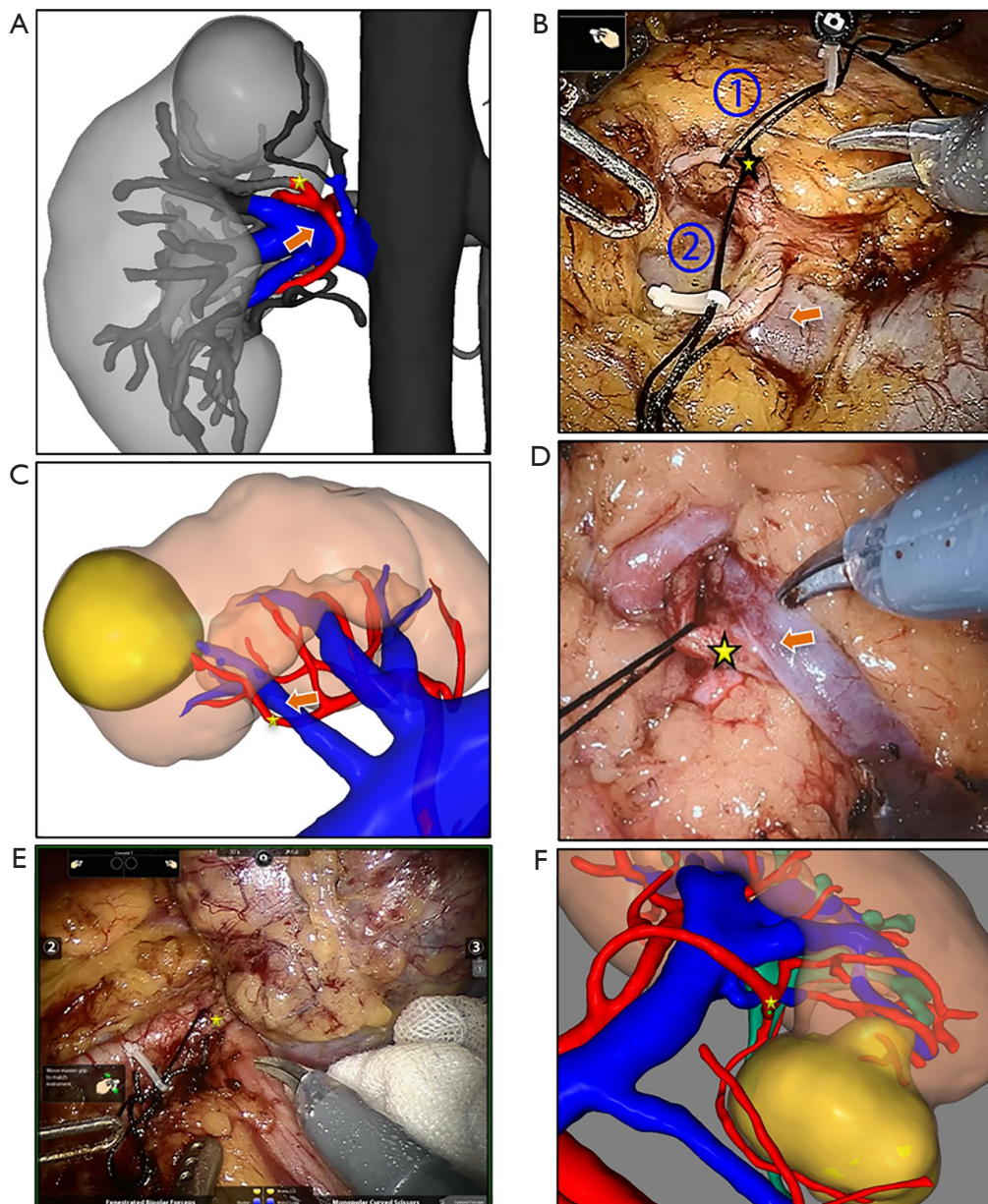
Anatomic landmark: renal vein and collecting system

Figure 4 The anatomic landmark function of surrounding organ. (A-D) The high-order tumor feeding artery is identified by accompanying vein which is positioned below and above the target artery. (E,F) Tumor's supply artery is identified by collecting system. Yellow pentagrams indicate tumor feeding artery; orange arrows indicate renal vein or collecting system; Dividing the telecentric and proximal (①③ and ②) end of artery by Sutures, anchored with a Hem-o-Lok clip.

to compare the accuracy and feasibility of pre-operative planning between H3DR- and CTA-guided surgery in the same patients. With the aid of this technology, it is possible not only to achieve minimal ischemic injury even when they have hidden feeding vessels, but also to avoid unwanted damage to surrounding organs during unnecessary separation steps. All these yield a potential improvement in the accuracy of the operative planning and an increase in MIRPCR, as well as a reduction in renal warm ischemia injury.

To sum up, with H3DR guidance, based on the specific anatomy of the intraparenchymal structures, both the excising and reconstructing portions of RALPN surgery could be optimized. Future evolution of this technology would be a simulation model that uses real-time surgical-region imaging to recognize and guide the operating doctors to the exact stenosis area during PN. Furthermore, more sophisticated computational techniques are becoming available, such as Artificial Intelligence-Aided Technology, will allow the dynamic deformations, to achieve accurate and fast anatomic dissection.

In combination, these improvements can lead to improved resection quality and suturing, resulting in fewer complications postoperatively and fewer adverse effects on the kidney, thus, helps to improve the development of RALPN.

Conclusions

For patients undergoing robotic/laparoscopic PN, in comparison with standard CTA-guided surgery, H3DR-guided surgery has higher accuracy and feasibility in controlling arterial branches supplying the tumor and intraoperative surgical navigation. Besides, it reduces the ischemic lesion area and simplifies vascular isolation steps, thus decreasing procedural difficulty.

Acknowledgments

Footnote

Reporting Checklist: The authors have completed the STROBE reporting checklist. Available at https://tau.amegroups.com/article/view/10.21037/tau-22-865/rc

Data Sharing Statement: Available at https://tau.amegroups.com/article/view/10.21037/tau-22-865/dss

Conflicts of Interest: All authors have completed the ICMJE

uniform disclosure form (available at https://tau.amegroups.com/article/view/10.21037/tau-22-865/coif). The authors have no conflicts of interest to declare.

Ethical Statement: The authors are accountable for all aspects of the work in ensuring that questions related to the accuracy or integrity of any part of the work are appropriately investigated and resolved. The study was conducted in accordance with the Declaration of Helsinki (as revised in 2013). Ethics was approved by Sun Yat-sen University Cancer Center Ethics Committee (approval number: XJS2018-005-01). Informed consent was taken from all the patients.

References

1. Volpe A, Blute ML, Ficarra V, et al. Renal Ischemia and Function After Partial Nephrectomy: A Collaborative Review of the Literature. Eur Urol 2015;68:61-74.

2. Badani KK, Kothari PD, Okhawere KE, et al. Selective clamping during robot-assisted partial nephrectomy in patients with a solitary kidney: is it safe and does it help? BJU Int 2020;125:893-7.

3. Desai MM, de Castro Abreu AL, Leslie S, et al. Robotic partial nephrectomy with superselective versus main artery clamping: a retrospective comparison. Eur Urol 2014;66:713-9.

4. Komninos C, Shin TY, Tuliao P, et al. Renal function is the same 6 months after robot-assisted partial nephrectomy regardless of clamp technique: analysis of outcomes for off-clamp, selective arterial clamp and main artery clamp techniques, with a minimum follow-up of 1 year. BJU Int 2015;115:921-8.

5. Rod X, Peyronnet B, Seisen T, et al. Impact of ischaemia time on renal function after partial nephrectomy: a systematic review. BJU Int 2016;118:692-705.

6. Rosen DC, Paulucci DJ, Abaza R, et al. Is Off Clamp Always Beneficial During Robotic Partial Nephrectomy?

A Propensity Score-Matched Comparison of Clamp Technique in Patients with Two Kidneys. J Endourol 2017;31:1176-82.

7. Ginzburg S, Uzzo R, Walton J, et al. Residual Parenchymal Volume, Not Warm Ischemia Time, Predicts Ultimate Renal Functional Outcomes in Patients Undergoing Partial Nephrectomy. Urology 2015;86:300-5.

8. Marconi L, Desai MM, Ficarra V, et al. Renal Preservation and Partial Nephrectomy: Patient and Surgical Factors. Eur Urol Focus 2016;2:589-600.

9. Maurice MJ, Ramirez D, Malkoç E, et al. Predictors of Excisional Volume Loss in Partial Nephrectomy: Is There Still Room for Improvement? Eur Urol 2016;70:413-5.

10. Simmons MN, Hillyer SP, Lee BH, et al. Functional recovery after partial nephrectomy: effects of volume loss and ischemic injury. J Urol 2012;187:1667-73.

11. Porpiglia F, Bertolo R, Amparore D, et al. Evaluation of functional outcomes after laparoscopic partial nephrectomy using renal scintigraphy: clamped vs clampless technique. BJU Int 2015;115:606-12.

12. Simone G, Gill IS, Mottrie A, et al. Indications, techniques, outcomes, and limitations for minimally ischemic and off-clamp partial nephrectomy: a systematic review of the literature. Eur Urol 2015;68:632-40.

13. Shao P, Qin C, Yin C, et al. Laparoscopic partial nephrectomy with segmental renal artery clamping: technique and clinical outcomes. Eur Urol 2011;59:849-55.

14. Shao P, Tang L, Li P, et al. Precise segmental renal artery clamping under the guidance of dual-source computed tomography angiography during laparoscopic partial nephrectomy. Eur Urol 2012;62:1001-8.

15. Abreu AL, Gill IS, Desai MM. Zero-ischaemia robotic partial nephrectomy (RPN) for hilar tumours. BJU Int 2011;108:948-54.

16. Alenezi A, Novara G, Mottrie A, et al. Zero ischaemia partial nephrectomy: a call for standardized nomenclature and functional outcomes. Nat Rev Urol 2016;13:674-83.

17. Cadeddu JA. "Zero Ischemia" Partial Nephrectomy: Novel Laparoscopic and Robotic Technique Editorial Comment. Journal of Urology 2011;186:77.

18. Gill IS, Patil MB, Abreu AL, et al. Zero ischemia anatomical partial nephrectomy: a novel approach. J Urol 2012;187:807-14.

19. Ng CK, Gill IS, Patil MB, et al. Anatomic renal artery branch microdissection to facilitate zero-ischemia partial nephrectomy. Eur Urol 2012;61:67-74.

20. Gill IS, Eisenberg MS, Aron M, et al. 1078 "ZERO-ISCHEMIA" partial nephrectomy: novel laparoscopic & robotic technique. 2011;59:128-34.

21. Mottrie A, De Naeyer G, Schatteman P, et al. Impact of the learning curve on perioperative outcomes in patients who underwent robotic partial nephrectomy for parenchymal renal tumours. Eur Urol 2010;58:127-32.

22. Wang Y, Ma X, Huang Q, et al. Comparison of robot-assisted and laparoscopic partial nephrectomy for complex renal tumours with a RENAL nephrometry score ≥7: peri-operative and oncological outcomes. BJU Int 2016;117:126-30.

23. Minervini A, Vittori G, Antonelli A, et al. Open versus robotic-assisted partial nephrectomy: a multicenter comparison study of perioperative results and complications. World J Urol 2014;32:287-93.

24. Zhao X, Lu Q, Ji C, et al. Trifecta outcomes of modified robot-assisted simple enucleation and standard robot-assisted partial nephrectomy for treating clinical T1b renal cell carcinoma. Transl Androl Urol 2021;10:1080-7.

25. Porpiglia F, Checcucci E, Amparore D, et al. Three-dimensional Augmented Reality Robot-assisted Partial Nephrectomy in Case of Complex Tumours (PADUA >= 10): A New Intraoperative Tool Overcoming the Ultrasound Guidance. European Urology 2020;78:229-38.

26. Porpiglia F, Fiori C, Checcucci E, et al. Hyperaccuracy Three-dimensional Reconstruction Is Able to Maximize the Efficacy of Selective Clamping During Robot-assisted Partial Nephrectomy for Complex Renal Masses. Eur Urol 2018;74:651-60.

27. Kutikov A, Uzzo RG. The R.E.N.A.L. nephrometry score: a comprehensive standardized system for quantitating renal tumor size, location and depth. J Urol 2009;182:844-53.

28. Moch H, Artibani W, Delahunt B, et al. Reassessing the current UICC/AJCC TNM staging for renal cell carcinoma. Eur Urol 2009;56:636-43.

29. Dindo D, Demartines N, Clavien PA. Classification of surgical complications: a new proposal with evaluation in a cohort of 6336 patients and results of a survey. Ann Surg 2004;240:205-13.

30. Thompson RH, Lane BR, Lohse CM, et al. Every minute counts when the renal hilum is clamped during partial

nephrectomy. Eur Urol 2010;58:340-5.
31. Shirk JD, Thiel DD, Wallen EM, et al. Effect of 3-Dimensional Virtual Reality Models for Surgical Planning of Robotic-Assisted Partial Nephrectomy on Surgical Outcomes: A Randomized Clinical Trial. JAMA Netw Open 2019;2:e1911598.

(English Language Editor: J. Jones)

Cite this article as: Wu C, Guo S, Zhuo S, Wang Y, Ye Y, Li Z, Mou Y, Yang X, Zhang Z, Dong P, Zhou F, Han H. Better specificity and less ischemia: three-dimensional reconstruction is superior to routine computed tomography angiography in navigation of super-selective clamping robot-assisted laparoscopic partial nephrectomy. Transl Androl Urol 2023;12(1):97-111. doi: 10.21037/tau-22-865